





Migrating Pyramidal Neurons Require DSCAM to Bypass the Border of the Developing Cortical Plate

Tao Yang,^{1,6} Macy W. Veling,¹  Xiao-Feng Zhao,² Nicholas P. Prin,¹ Limei Zhu,¹ Ty Hergenreder,¹ Hao Liu,^{1,2} Lu Liu,³ Zachary S. Rane,¹ Masha G. Savelieff,¹  Peter G. Fuerst,⁴ Qing Li,³  Kenneth Y. Kwan,⁵ Roman J. Giger,² Yu Wang,⁶ and  Bing Ye^{1,2}

¹Life Sciences Institute, University of Michigan, Ann Arbor, Michigan 48109, ²Department of Cell and Developmental Biology, University of Michigan, Ann Arbor, Michigan 48109, ³Internal Medicine, Hematology/Oncology, University of Michigan, Ann Arbor, Michigan 48109, ⁴Department of Biological Sciences, University of Idaho, Moscow, Idaho 83844, ⁵Department of Human Genetics, University of Michigan, Ann Arbor, Michigan 48109, and ⁶Department of Neurology, University of Michigan, Ann Arbor, Michigan 48109

During mammalian neocortex development, nascent pyramidal neurons migrate along radial glial cells and overtake earlier-born neurons to terminate at the front of the developing cortical plate (CP), leading to the outward expansion of the CP border. While much has been learned about the cellular and molecular mechanisms that underlie the migration of pyramidal neurons, how migrating neurons bypass the preceding neurons at the end of migration to reach their final positions remains poorly understood. Here, we report that Down syndrome cell adhesion molecule (DSCAM) is required for migrating neurons to bypass their postmigratory predecessors during the expansion of the upper cortical layers. DSCAM is a type I transmembrane cell adhesion molecule. It has been linked to Down syndrome through its location on Chromosome 21 trisomy and to autism spectrum disorders through loss-of-function mutations. *Ex vivo* time-lapse imaging demonstrates that DSCAM is required for migrating neurons to bypass their postmigratory predecessors, crossing the CP border to expand the upper cortical layers. In *DSCAM*-deficient cortices, migrating neurons stop prematurely under the CP border, leading to thinner upper cortical layers with higher neuronal density. We further show that DSCAM weakens cell adhesion mediated by N-cadherin in the upper cortical plate, allowing migrating neurons to traverse the CP border and expand the CP. These findings suggest that DSCAM is required for proper migratory termination and final positioning of nascent pyramidal neurons, which may provide insight into brain disorders that exhibit thinner upper layers of the cerebral cortex without neuronal loss.

Key words: cell adhesion; cortex development; DSCAM; migration; pyramidal neuron; termination

Significance Statement

Newly born neurons in the developing mammalian neocortex migrate outward toward the cortical surface, bypassing earlier born neurons to expand the developing cortex. How migrating neurons bypass the preceding neurons and terminate at the front of the expanding cortex remains poorly understood. We demonstrate that Down syndrome cell adhesion molecule (DSCAM), linked to Down syndrome and autism spectrum disorder, is required by migrating neurons to bypass their postmigratory predecessors and terminate migration in the outwardly expanding cortical layer. Migrating neurons deficient in *DSCAM* stop prematurely, failing to expand the cortex. We further show that DSCAM likely mediates migratory termination by weakening cell adhesion mediated by N-cadherin.

Received May 11, 2021; revised May 24, 2022; accepted May 27, 2022.

Author contributions: T.Y. and B.Y. designed research; T.Y., M.W.V., X.-F.Z., N.P.P., L.Z., T.H., H.L., L.L., Q.L., R.J.G., and Z.S.R. performed research; M.G.S., P.G.F., K.Y.K., and Y.W. contributed unpublished reagents/analytic tools; T.Y. and N.P.P. analyzed data; T.Y., M.G.S., and B.Y. wrote the paper.

This study was supported by National Institutes of Health Grants R01-EB-028159 and R21-NS-094091; a Seed Grant from the Brain Research Foundation; the Protein Folding Disease Initiative of the University of Michigan to B.Y.; and a University of Michigan Mcubed pilot grant to B.Y., Y.W., and K.Y.K. The content of this work is solely the responsibility of the authors and does not necessarily represent the official views of the National Institutes of Health. We thank Dr. Andrew Garrett for critical feedback on the work, Dr. Joshua Sanes for sharing HEK293NC and TA cell lines, and Drs. Robert Reiter and Joyce Yamshiro for sharing anti-N-cadherin antibodies and related information.

The authors declare no competing financial interests.

Correspondence should be addressed to Bing Ye at bingye@umich.edu.

<https://doi.org/10.1523/JNEUROSCI.0997-21.2022>

Copyright © 2022 the authors

Introduction

During mammalian neocortical development, nascent pyramidal neurons, born in the ventricular or subventricular zone (SVZ), migrate along radial glial cells to generate cortical layers. As they migrate, the later-born pyramidal neurons overtake earlier-born neurons to terminate at the border of the cortical plate (CP), leading to an “inside-out” pattern of cortical layer formation. Despite intense interest in this important process of cortical development, how migrating neurons bypass the preceding neurons at the end of migration to locate their final positions remains poorly understood.

Neuronal migration defects in mutant mice have provided insights into neuronal positioning during cortical genesis. In

Reeler (*reelin*) and *Scrambler* [*Disabled 1 (Dab1)*] mice, migrating neurons do not follow the inside-out layer formation, resulting in an inverted cerebral cortex (Sheldon et al., 1997; D'Arcangelo, 2006). In *reelin*-deficient or *Dab1*-deficient mice, postmigratory neurons remain attached to the radial glia. Cell adhesion molecules regulate the neuronal detachment from radial glia (Anton et al., 1996). For example, $\alpha 3$ integrin expression in the upper CP differs in wild-type and *Scrambler* mice, and Reelin blocks $\alpha 3$ integrin expression at the top of the CP to facilitate neuron detachment (Sanada et al., 2004). SPARC-like 1 is also specifically expressed in the upper CP and may modulate neuronal adhesion to promote detachment (Gongidi et al., 2004). While these studies demonstrate that proper exit from radial migration is critical for the inside-out formation of cortical layers (Pinto-Lord et al., 1982; Sanada et al., 2004), how later-born neurons bypass the postmigratory preceding neurons at the CP border has not been characterized.

Down syndrome cell adhesion molecule (DSCAM) is a type I transmembrane cell adhesion molecule of the Ig superfamily (Yamakawa et al., 1998; Agarwala et al., 2000). Loss-of-function *DSCAM* mutations in human have been linked to neurobehavioral conditions, such as autism spectrum disorder (Turner et al., 2016; Wang et al., 2016; Narita et al., 2020), highlighting the importance of DSCAM in neurodevelopment. The *Drosophila* homolog of DSCAM, *Dscam1*, mediates dendrite or axon self-avoidance (Hughes et al., 2007; Matthews et al., 2007; Soba et al., 2007), a process that requires remarkable molecular diversity. Alternative splicing of the extracellular ectodomain of *Drosophila Dscam1* can, in theory, generate >19,000 isoforms (Schmucker et al., 2000; Hattori et al., 2009). Furthermore, *Drosophila Dscam1* expression levels dictate neuronal axon terminal growth independent of its ectodomain diversity (Kim et al., 2013).

Mammalian DSCAM does not possess ectodomain diversity like its *Drosophila* homolog (Schmucker and Chen, 2009). Rather, in mammals, neurite self-avoidance is mediated through protocadherin diversity (Zipursky and Sanes, 2010; Lefebvre et al., 2012). DSCAM also contributes to neurite self-avoidance in mammals in a fashion that does not require large molecular diversity. This is achieved by masking the cell adhesion mediated by cadherins (Garrett et al., 2018). For instance, several *DSCAM*^{-/-} mutants exhibit retinal mosaic defects in mice, with excessive soma adhesion and process fasciculation (Fuerst et al., 2008, 2009, 2010). Intercellular DSCAM interaction decreases cell adhesion through masking cadherins and consequently promotes self-avoidance. DSCAM also regulates migrating neuron detachment from the ventricular surface in the midbrain (Arimura et al., 2020). Whether DSCAM is involved in cortical development remains poorly unknown.

In this study, we used *ex vivo* time-lapse imaging to demonstrate at the single-neuron resolution that DSCAM is required for migrating nascent neurons destined to upper cortical layers to bypass their postmigratory predecessor and migrate across the CP to expand the cortical layer. Migrating neurons deficient in *DSCAM* prematurely stops at the CP border together with their postmigratory predecessors. Thus, *DSCAM*-deficient neurons fail to expand the upper cortical layers, leading to a thinner and denser cortical layer. Our results show that DSCAM masks cell adhesion mediated by N-cadherin in the upper cortical plate, facilitating radial migrating neurons to bypass the border of the developing CP. These findings suggest that DSCAM is required for proper migratory termination and final positioning of nascent pyramidal neurons, which may provide insight into brain

disorders that exhibit thinner upper layers of cerebral cortex without neuronal loss (Arnold and Trojanowski, 1996).

Materials and Methods

Mice. In this study, we used *DSCAM*^{2j/2j} mutant mice for *DSCAM* loss-of-function studies because it does not produce a protein product and mice survive postnatally on the inbred background that it arose on (Fuerst et al., 2010). The *DSCAM*^{2j} allele harbors a spontaneous 4 bp duplication in exon 19, leading to a frameshift and loss of function. The 8-week-old *DSCAM*^{2j/+} mice (hereafter referred to as *DSCAM*^{+/-}) were crossed to generate *DSCAM*^{+/+}, *DSCAM*^{+/-}, and *DSCAM*^{-/-} mice. The *nestin-CreERT2* mouse [C57BL/6-Tg(Nes-creERT2)KEiscl/J; stock #016261, The Jackson Laboratory; Lagace et al., 2007], under the *nestin* promoter, expresses tamoxifen-induced Cre recombinase in adult and developing mouse brains, including neural progenitor cells (NPCs). The Ai14 mouse [*GeneTrap* B6.Cg-Gt(ROSA)26Sor^{tm14(CAG-tdTomato)Hze/J}]; stock #007914, The Jackson Laboratory; Madisen et al., 2010] expresses the red fluorescent protein (RFP) tdTomato in a Cre-dependent fashion. *DSCAM*^{+/-} animals were bred into *nestin-CreERT2* and Ai14 mice to generate *DSCAM*^{-/-}/*nestin-CreERT2*/CAG-tdTomato progeny with tamoxifen-inducible *nestin*-promoter-restricted tdTomato expression in NPCs. tdTomato was induced by tamoxifen injection into dams bearing embryonic day 14.5 (E14.5) embryos and was expressed by all NPC progeny cells.

All mice were handled in accordance with a protocol approved by the Institutional Animal Care and Use Committee at the University of Michigan. The mice were housed in a dedicated temperature-controlled (20°C) animal facility with a 12 h light/dark cycle maintained by the Unit for Laboratory Animal Medicine at the University of Michigan. The mice were housed in groups of no more than five per cage and were provided regular chow and water *ad libitum*. Their health was monitored onsite by a dedicated veterinarian staff.

In utero electroporation of mouse embryos. *In utero* electroporation (IUE) was performed as previously described with some modifications (Sun et al., 2010; Yang et al., 2012). Pregnant female mice (E14.5) were anesthetized with isoflurane, and an incision was made to expose the embryos while still within the uterus. A plasmid DNA solution (~2–3 μ g/ μ l) containing 0.01% (w/v) Fast Green dye was injected (~1–2 μ l) into the right side of the lateral ventricle of each embryo brain using a glass micropipette. Each embryo head, still within the uterus, was placed between the leads of a Tweezertrode Electrode system (diameter, 5 mm; BTX, Harvard Bioscience) and administered five electrical pulses (50 V, 50 ms duration, 950 ms intervals) using an electroporator (ECM830, Harvard Bioscience). Embryos were returned to the pregnant female, and the muscle and skin were sutured, respectively. The pregnant female was monitored until she revived and was administered carprofen (5 mg/kg, i.p.) for pain management.

Genotyping embryonic tissues. Embryo genomic DNA was purified for genotyping by digesting tail tissue in 300 μ l of TES buffer (50 mM Tris, pH 8.0, 0.5% SDS, 0.1 M EDTA, in 1 \times PBS) with proteinase K overnight. Then, 5 M NaCl (160–200 μ l) was added before centrifugation to remove precipitates. Next, isopropanol (180 μ l) was added to the 300 μ l of supernatant to precipitate the DNA. The DNA pellets were washed with 500 μ l of 70% ethanol before dissolving in 20 μ l of water. DNA flanking the *DSCAM*^{2j} mutation were amplified by PCR (forward primer: 5'-gccctgtggtatttctggtgtg-3'; reverse primer: 5'-gatgggcaaatgtcaaggtcaaa-3'). The PCR product was sequenced with either primer to verify the presence of the mutation.

Live-cell time-lapse confocal microscopy of brain sections. Brain slice culture and time-lapse confocal imaging were performed as previously described (Yang et al., 2012). Brains of E19.5 embryos were coronally sectioned in ice-cold artificial cortical spinal cord fluid on a vibratome (Leica Microsystems) into 300 μ m slices. Brain slices were then immersed in DMEM and continuously perfused with DMEM bubbled with 95% O₂ and 5% CO₂ at 37°C on the microscope stage. Time-lapse imaging was performed using confocal microscopy (model TCS SP5, Leica) with an HC Fluotar L 25 \times /0.95 W VISIR immersion objective lens at 5 min intervals for a 15 h duration. The embryos were genotyped as described above.

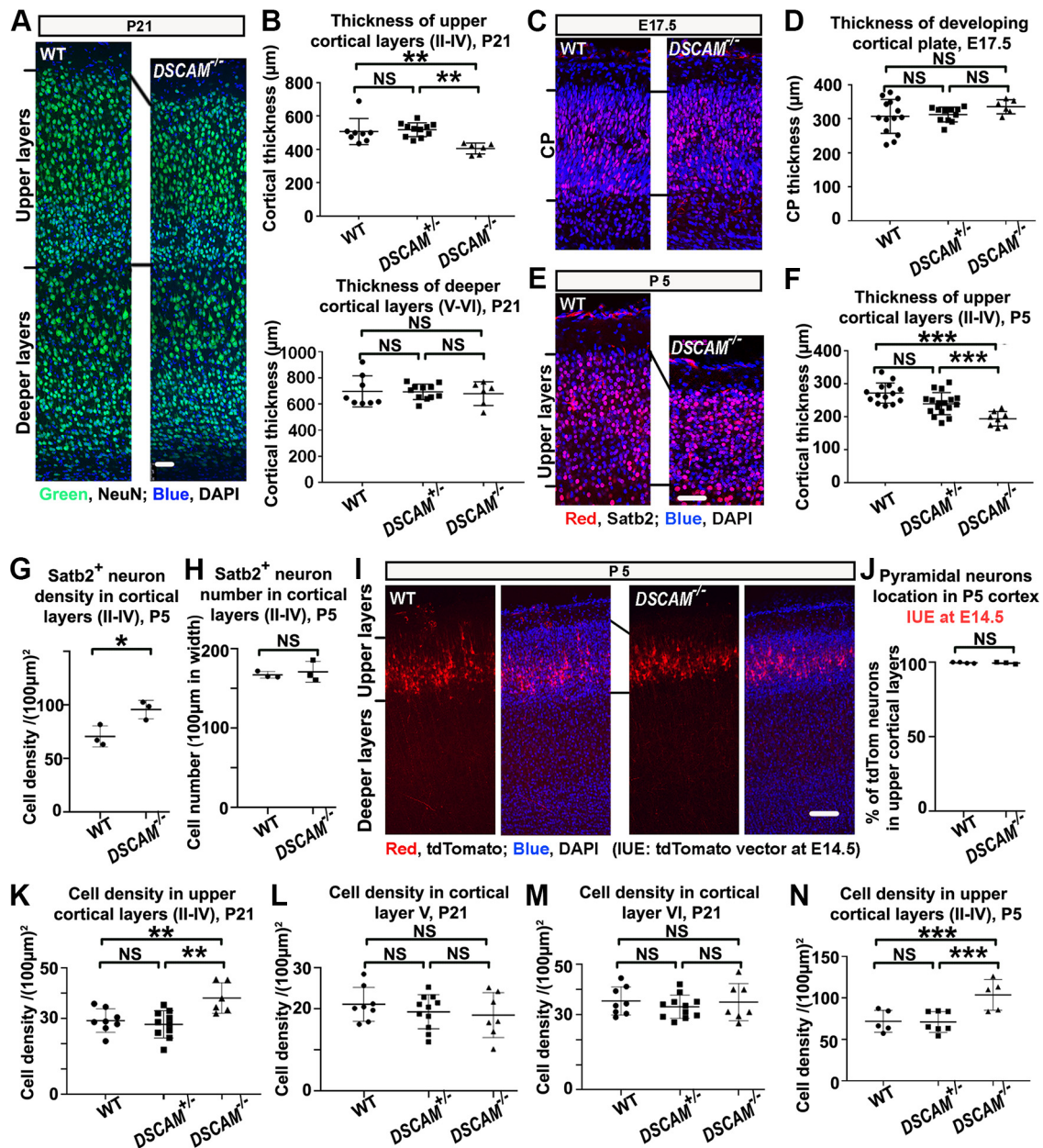


Figure 1. DSCAM is required for expanding the developing upper cortical layers. **A**, Immunostaining of NeuN (green channel) in wild-type (WT) and *DSCAM*^{-/-} cortex at P21 counterstained with DAPI (blue channel). **B**, Quantification of the thickness of cortical layers in WT, *DSCAM*^{+/-}, and *DSCAM*^{-/-} at P21. Top, Upper cortical layers. Bottom, Deeper cortical layers. One-way ANOVA followed by *post hoc* Student's *t* test. NS, Not significant. $p > 0.05$; $**p < 0.01$. **C, E**, Immunostaining of Satb2 (red channel) in WT and *DSCAM*^{-/-} cortices counterstained with DAPI (blue) at E17.5 (**C**) and P5 (**E**). **D, F**, Quantification of the thickness of developing cortices in WT, *DSCAM*^{+/-}, and *DSCAM*^{-/-} at E17.5 (**D**) and P5 (**F**). One-way ANOVA followed by *post hoc* Student's *t* test. NS, $p > 0.05$; $***p < 0.001$. **G, H**, Quantification of Satb2⁺ cell densities (**G**) and total number (**H**) in upper cortical layers (II–IV) at P5. Mann–Whitney *U* test. NS, $p > 0.05$; $*p < 0.05$. **I**, tdTomato⁺ pyramidal neurons (red) labeled by *in utero* electroporation at E14.5 locate in the upper cortical layers (labeled by DAPI staining, blue) at P5. **J**, Quantification of the percentage of tdTomato⁺ neurons in upper cortical layers in WT and *DSCAM*^{-/-} at P5. Fisher's exact test. NS, $p > 0.05$. **K–N**, Quantification of cell densities in upper cortical layers (II–IV), layer V, layer VI at P21, and upper cortical layers at P5. One-way ANOVA followed by *post hoc* Student's *t* test. NS, $p > 0.05$; $**p < 0.01$; $***p < 0.0001$. Scale bar, 50 μm.

Fluorescence immunohistochemistry of brain sections. Brains were fixed by 4% paraformaldehyde (PFA; in PBS) overnight. Then, brains were immersed in 30% sucrose overnight, followed by embedding in optimal cutting temperature (O.C.T.) media (Tissue-Tek, Sakura), and freezing at -80°C . Brains were sectioned coronally at 100 μm thickness, permeabilized with 0.1% Triton X-100 in PBS, blocked with 2% donkey serum in PBS, and incubated overnight at 4°C with primary antibodies. The antibodies used are as follows: (1) mouse anti-NeuN (1:1000; catalog #ab104224, Abcam); (2) rabbit anti-Satb2 (1:1000; catalog #ab92446, Abcam); (3) rabbit anti-Tbr1 (1:1000; catalog #ab31940, Abcam); (4) rabbit anti-Ki67 (1:1000; catalog #ab15580, Abcam); (5) rabbit anti-SOX2 (1:1000; catalog #ab5603, Chemicon); or (6) rabbit anti-Cleaved

Caspase-9 (1:500; catalog #PA5-17 913, Thermo Fisher Scientific). Sections were rinsed and probed with secondary antibodies against mouse or rabbit (1:500; Jackson ImmunoResearch). The brain sections were then counterstained with DAPI, rinsed, and mounted in 50% glycerol before visualization. Images were captured using an SP5 confocal microscope (Leica).

RNA in situ hybridization of brain sections. *DSCAM* mRNA *in situ* hybridization (ISH) was conducted using previously published probe sequences (Fuerst et al., 2009) and from the Genepaint website. Probe sequences were amplified from *DSCAM* cDNA (catalog #18737, Addgene; Yamagata and Sanes, 2008) and cloned into a pTOPO vector. DIG-labeled cRNA probes were generated using a DIG RNA labeling kit (Roche), as previously described (Lin et al., 2017). Briefly, DIG-labeled cRNA probes

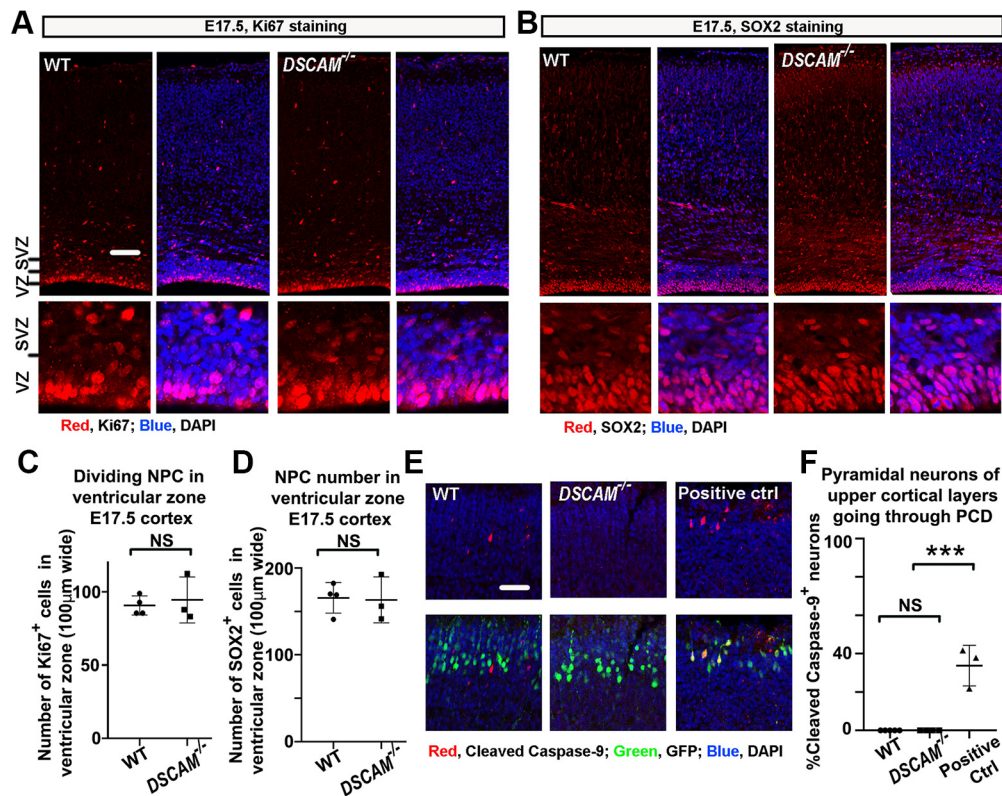


Figure 2. Loss of *DSCAM* does not affect the number of neural progenitors and that of cells undergoing programmed cell death in the neocortex. *A, B*, Immunostaining of the proliferation marker Ki67 (*A*) and the marker Sox2 of the neural progenitor cell (*B*, red channel) in wild-type (WT) and *DSCAM*^{−/−} cortices at E17.5. The cortical slices were counterstained with DAPI (blue channel). Scale bar, 50 µm. *C, D*, Quantification of the total number of neural progenitors in the ventricular zone in WT and *DSCAM*^{−/−} at E17.5. Student’s *t* test. *NS* *p* > 0.05. *E*, Immunostaining of cleaved Caspase-9 (red channel)—which indicates activated Caspase-9—in WT and *DSCAM*^{−/−} cortical slices counterstained with DAPI (blue) at E19.5. Upper cortical neurons were labeled by transfecting an EGFP-expressing plasmid (pCAGGS-IRES-EGFP) via IUE at E14.5. The programmed cell death in the positive controls was caused by MUNC18-1 knockout (Verhage et al., 2000). *F*, Quantification of the cells positive for cleaved Caspase-9 in upper cortical layers of WT, *DSCAM*^{−/−}, and the positive control in 100-µm-wide cerebral cortices at E19.5. Shown are the percentage of GFP⁺ neurons that were also positive for cleaved Caspase-9 in the total number of GFP⁺ neurons. One-way ANOVA followed by *post hoc* Mann–Whitney *U* test. *NS* *p* > 0.05, ****p* < 0.0001.

were generated by *in vitro* transcription from the *DSCAM* cDNA template. ISH was performed on fresh-frozen mouse brain sections mounted on microscope slides, which were fixed, permeabilized by proteinase K, incubated with DIG-labeled cRNA probes, rinsed, and incubated with anti-DIG-AP (alkaline phosphatase) antibody (Roche). The signal was visualized by an AP substrate NBT (nitro-blue tetrazolium chloride)/BCIP (5-bromo-4-chloro-3'-indolylphosphate p-toluidine salt; Roche).

Cell brain slice adhesion test. HEK293NC (no N-cadherin expressed) and TA (with N-cadherin expressed) cells (Yamagata and Sanes, 2018) were cultured in DMEM with 10% FBS in a humidified cell culture hood at 37°C and 5% CO₂. N-cadherin (1.5 µg plasmid; catalog #18870, Addgene; Nechiporuk et al., 2007) or N-cadherin (1.5 µg plasmid)/*DSCAM* (0.5 µg plasmid) were transfected respectively with Lipofectamine (Thermo Fisher Scientific) into HEK293NC and TA cells (Yamagata and Sanes, 2018). Transfected HEK293 cells were incubated in a humidified cell culture hood at 37°C and 5% CO₂ for 2 d. E19.5/postnatal day 0 (P0) brains were dissected and sectioned into 300 µm brain slices. To neutralize N-cadherin-mediated cell adhesion in HEK293NC cells expressing N-cadherin, 50 µl mouse anti-N-cadherin antibody (GC-4 clone; C3865, Sigma-Aldrich; RRID:AB_262097; Wallerand et al., 2010) was added to the isolated HEK293 cells for 10 min before they were added to cortical slices. The cortical slices were attached to the bottom of wells of a 24-well plate. Isolated HEK293 cells were incubated with the cortical slices for 2 h. After that, the brain slices were rinsed three times with 1 × PBS to remove unattached cells and debris. Then, the brain slices and attached HEK293 cells were fixed with 4% PFA. Cell numbers were counted within each layer, the marginal zone (MZ), upper CP, and lower CP. The percentage of cells in each layer of the total cell number was calculated to represent the attaching ability introduced by N-cadherin.

To test the adhesion of primary neurons to the cortical plate, neurons were labeled with RFP expressed by PBCAG-mRFP (catalog #40996, Addgene) by IUE at E14.5. Then, at E19.5 the transfected cortices were dissected and triturated to dissociate the neurons. The neurons were incubated on wild-type cortical slices for 2 h. The remaining steps are the same as those for the HEK293 cortical slice adhesion assay.

Western blotting. HEK293 cells were lysed in 2 × sample buffer, sonicated, and boiled at 95°C for 5 min. Samples were then loaded onto 4–20% SDS-PAGE gels (catalog #4561093, BIO-RAD) for electrophoresis and transferred to nitrocellulose membrane (Novex). The membranes were blocked in 10% milk in 1 × PBS (with 0.1% Triton X-100), then incubated overnight at 4°C with the following primary antibodies: (1) goat anti-*DSCAM* antibody (1:100; catalog #AF3666, R&D Systems); (2) rabbit anti-N-cadherin (1:2000; catalog #ab18203, Abcam); or (3) mouse anti-β-actin (1:10,000; catalog #AM4302, Thermo Fisher Scientific). After washes, the membranes were incubated with blocking buffer containing HRP-conjugated secondary antibodies (BIO-RAD) for 2 h at room temperature. The signal was developed in ChemiDoc MP imager and quantified using ImageJ software. The signal of N-cadherin bands, β-actin bands, and background were measured with ImageJ.

Statistical analysis. Data were analyzed using GraphPad Prism 8. The types of statistical tests are shown in figure legends. All experiments were quantified in double-blind fashion so that the person who quantified the images did not know the genotypes or transfection plasmids.

Results

DSCAM is required for expanding upper cortical layers

To examine the contribution of *DSCAM* to cortical development, we compared the cortical histology of homozygous *DSCAM*^{2/2}

mice (referred to as *DSCAM*^{-/-} here on) and their wild-type and heterozygous littermates. Previous studies have shown that *DSCAM*^{2j} is a protein-null allele (Schramm et al., 2012; de Andrade et al., 2014). Fluorescence immunohistochemistry was performed on coronal brain sections from young adult mice at P21 using an antibody against NeuN, a pan-neuronal marker. The upper cortical layers (II–IV) were 21% thinner in *DSCAM*^{-/-} cortices compared with wild-type or heterozygous cortex (Fig. 1*A,B*, top panels). Surprisingly, the deeper cortical layers (V–VI) were unaffected (Fig. 1*A,B*, bottom panels). These results suggest that *DSCAM* is required for expanding the thickness of upper cortical layers. Formation of the upper cortical layers begins after E18.5 through radial migration of pyramidal neurons (Molyneux et al., 2007) and approaches completion at approximately P5 (Caviness, 1982; Supèr et al., 2000). Therefore, we determined whether *DSCAM* was required for proper cortical thickness during this developmental window. At E17.5, the CP thickness in *DSCAM*^{-/-} cortex was comparable to wild-type or *DSCAM*^{+/-} cortex (Fig. 1*C,D*), whereas at P5, *DSCAM*^{-/-} upper cortex was 25% thinner than wild-type or heterozygous cortex (Fig. 1*E,F*). These findings were further confirmed by immunostaining with an antibody against *Satb2*, a marker for neurons in cortical layers II–IV (Britanova et al., 2008). The density of *Satb2*⁺ neurons in *DSCAM*^{-/-} cortex was 26% higher than in wild-type cortex (Fig. 1*G*). However, the total number of *Satb2*⁺ neurons were similar between *DSCAM*^{-/-} and wild-type cortices (Fig. 1*H*). Thus, examining a wider developmental window further confirms that *DSCAM* is required for expanding the upper cortical layers.

DSCAM is required for neuronal dispersion in developing upper cortical layers

Defective radial migration distributes neurons to the incorrect layer, which could cause a thinner cortex (Rakic, 1988; Dobyns and Truwit, 1995). The thinner cortical layers that we observed in *DSCAM*^{-/-} mice could similarly arise from defective radial migration that mistakenly redirects neurons destined to the upper cortical layers to the deep cortical layers. To test this possibility, we used IUE in E14.5 embryos to introduce a tdTomato expression vector into dorsal NPCs, which give rise to pyramidal neurons (Ayala et al., 2007). The progeny neurons of these NPCs radially migrate and differentiate into pyramidal neurons in the upper cortical layers during E17.5 to P5 (Molyneux et al., 2007). We examined the cortices at P5, after radial migration had occurred, and only detected tdTomato neurons in the upper cortical layers in both wild-type and *DSCAM*^{-/-} cortex (Fig. 1*I, J*). This result demonstrates that lack of *DSCAM* does not prevent pyramidal neurons from migrating to the upper cortical layers through radial migration.

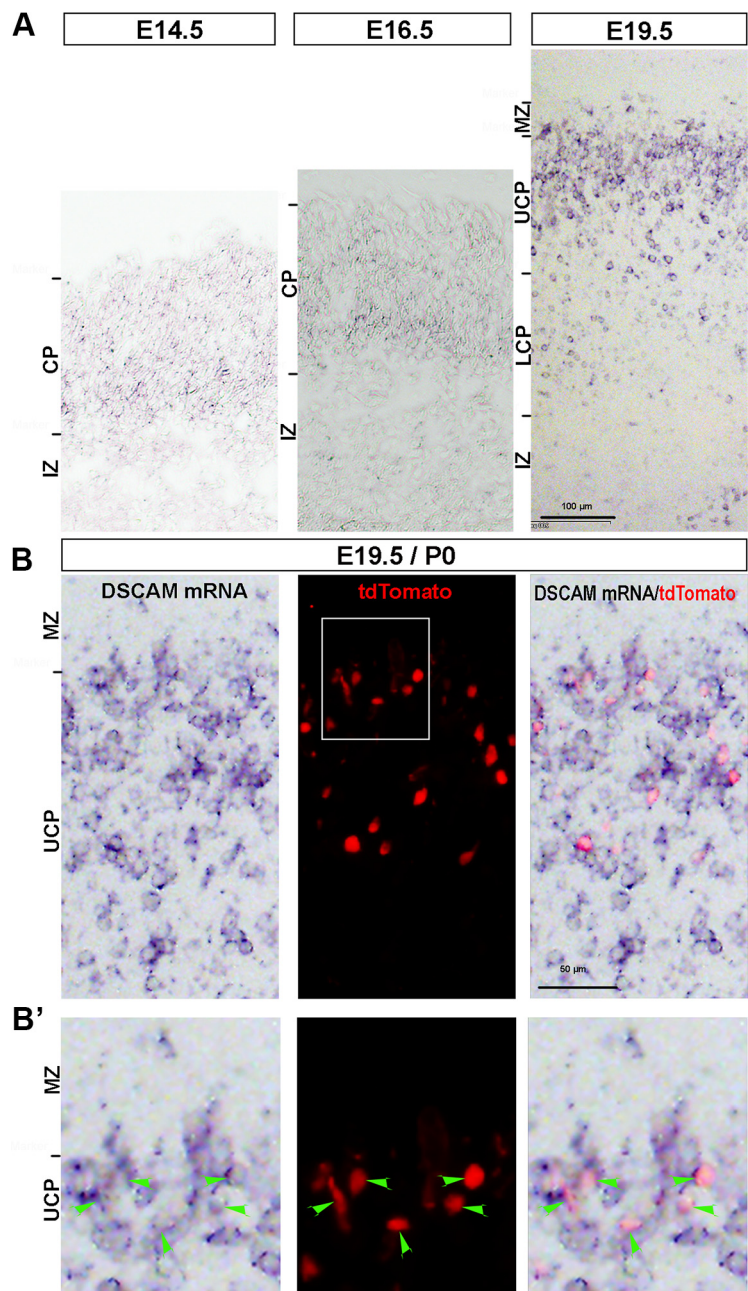


Figure 3. *DSCAM* is preferentially expressed in radial migrating neurons in the upper cortical plate. **A**, *DSCAM* mRNA *in situ* hybridization in developing WT cortices at E14.5 (left), E16.5 (middle), and E19.5 (right). IZ, Intermediate zone; LCP, lower cortical plate; UCP, upper cortical plate; MZ, marginal zone. Scale bar, 100 μ m. **B**, *DSCAM* mRNA is expressed in all tdTomato⁺ neurons, which are destined to the upper cortical layers in WT cortices at E19.5. Scale bar, 50 μ m. **B'**, Enlarged image of the boxed area in **B**; green arrowheads point to individual neurons. Left, *DSCAM* mRNA ISH. Middle, tdTomato. Right, Merge.

Alternatively, a thinner neocortex may also arise from the birth of fewer neurons. To assess whether this occurs in *DSCAM*^{-/-} cortex, we quantified the neuronal density from immunoreactivity to NeuN in the upper cortical layers at P5 and P21. The density of neurons in layers II–IV was >30% higher in *DSCAM*^{-/-} cortex compared with wild-type and heterozygous cortex (Fig. 1*K,N*; also see Fig. 1*G*). On the other hand, the neuronal density in deeper layers in *DSCAM*^{-/-} cortex was comparable to wild-type and heterozygotes cortex (Fig. 1*L,M*). The number of neural progenitors in the ventricular zone did not differ between *DSCAM*^{-/-} and wild-type at E17.5, as suggested by

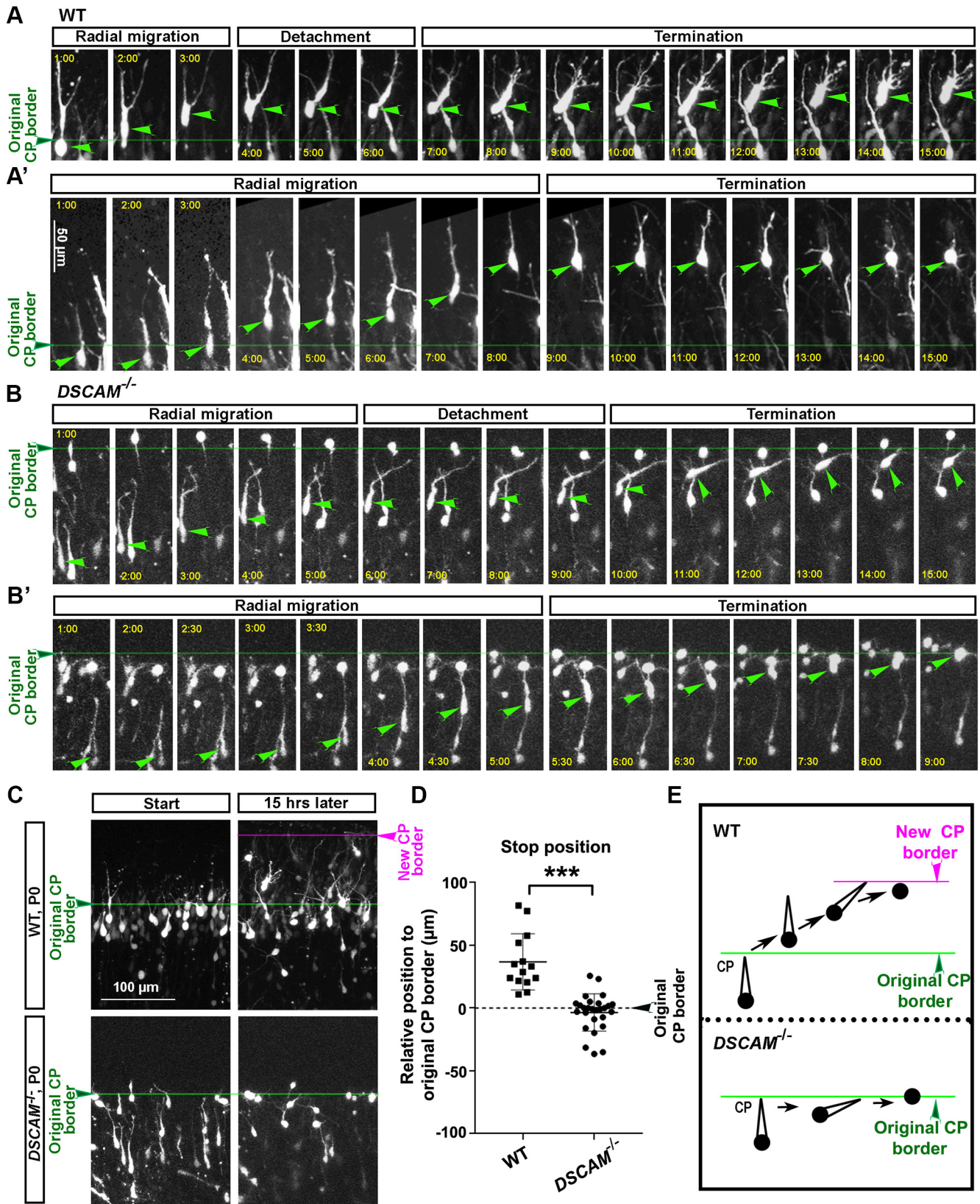


Figure 4. DSCAM is required for migrating neurons to bypass the CP border. **A, A'**, Cellular behaviors at the termination phase of radially migrating neurons. Representative time-lapse images of tdTomato⁺ neurons in WT cortices at E19.5. The images show several stages of migration. Neurons with a bipolar morphology and a thick leading process migrate radially to the CP border. They then extend multiple dynamic processes and, as migration terminates, retract the thick leading process. **A**, A representative neuron migrates laterally after radial migration. **A'**, A representative neuron stops immediately after radial migration. One hour per frame. The temporary CP border at the beginning of time-lapse imaging represented by a green horizontal line. Green arrowheads point to the soma of migrating neurons. Scale bar, 50 μ m. **B, B'**, Representative time-lapse images of tdTomato⁺ neurons in *DSCAM*^{-/-} cortices at E19.5. **B**, A representative neuron migrates laterally after radial migration. One hour per frame. **B'**, A representative neuron stops immediately after radial migration; 0.5 h/frame. **C, D**, The wild-type, but not *DSCAM*^{-/-}, cortices (P0) expanded during the course of the time-lapse imaging. **C**, Representative images. Left panels, The start point of the time lapse (E19.5/P0). Right panels, The same

immunostaining with the neural progenitor cell marker SOX2 and cell proliferation marker Ki67 (Graham et al., 2003; Tsai et al., 2005; Fig. 2A–D). Moreover, immunostaining with the marker for active caspase signaling suggests that programmed cell death was not altered at E19.5/P0 in the *DSCAM*^{-/-} cortex (Zou et al., 1999; Fig. 2E,F). These results demonstrate that the thinner upper cortical layers II–IV in *DSCAM*^{-/-} cortex does not result from fewer neurons. Rather, a similar number of pyramidal neurons are generated in *DSCAM*^{-/-} versus wild-type cortex, but these *DSCAM*^{-/-} neurons fail to disperse, leading to a thinner but denser upper cortical layer.

DSCAM is expressed in radially migrating neurons targeting the upper cortical layers

Since DSCAM is required for neuronal dispersion to the upper cortical layer, we sought to determine whether DSCAM was expressed in neurons that were destined to cortical layers II–IV. Since there are no reliable antibodies against mouse DSCAM for immunohistochemistry, we used RNA ISH to investigate *DSCAM* mRNA expression in the developing cortex. The upper cortical layer begins to develop at approximately E18.5; therefore, we performed RNA ISH on wild-type cortex at earlier time points, E14.5 and E16.5, and at a later time point, E19.5/P0. We found that *DSCAM* mRNA levels were low in the CP at E14.5 and E16.5 (Fig. 3A) but increased significantly in the upper CP at E19.5/P0 (Fig. 3A). These results indicate that increased *DSCAM* expression coincides with the formation of the upper cortical layers.

A salient difference between the later (E19.5/P0; high *DSCAM* expression) and earlier (E14.5 and E16.5; low *DSCAM* expression) time points that we examined is that nascent pyramidal neurons of upper cortical layers will have radially migrated and accumulated in the upper CP by the E19.5/P0 but not E14.5 and E 16.5 time points, since the upper cortical layer forms at approximately E18 onward. Therefore, we further examined whether *DSCAM* mRNA was expressed in these nascent neurons. We achieved this by genetically labeling NPCs at E14.5, which gives rise to the pyramidal neurons of the upper cortical layers, with tdTomato, and performing *DSCAM* mRNA ISH. We observed that *DSCAM* mRNA was expressed in all tdTomato⁺ neurons at E19.5/P0 (Fig. 3B,B'), which suggests that DSCAM is expressed in those nascent pyramidal neurons destined to the upper cortical layers.

DSCAM is required for newly incoming neurons to bypass their postmigratory predecessors at the CP border

Since DSCAM is expressed by radially migrating neurons but its deficiency does not cause defective radial migration, we sought to determine whether DSCAM was instead involved in the termination of migration. We used time-lapse live imaging to investigate this possibility. We fluorescently labeled radially migrating neurons in wild-type and *DSCAM*^{-/-} cortex by transfecting NPCs with a tdTomato expression vector by IUE at E14.5. In mice, neurons born at E14.5 establish the cortical layer IV at E19/P0 (Kwan et al., 2012); therefore, we performed time-lapse imaging around the CP border at E19.5/P0.

←

cortical regions 15 h later. The CP expanded in WT (top) but not in *DSCAM*^{-/-} (bottom). The original cortical border is indicated by a green line, and the new CP border 15 h later is indicated by a magenta line. Scale bar, 100 μ m. **D**, Quantification of the final positions of the migrating neurons. "0" is the CP border at the beginning of the time-lapse imaging. Student's *t* test, ****p* < 0.0001. **E**, Schematic of the termination stage of neuronal migration.

In wild-type cortex, neurons migrated across the CP with a bipolar morphology and a leading process oriented radially (Fig. 4A, 1:00–4:00 h, A', 1:00–8:00 h). After crossing the original CP boundary, which is delineated by the lower cell density in MZ, the neurons ceased migrating radially. At this stage, neurons either continued migrating nonradially a short distance to their final stopping position (Fig. 4A) or immediately halted without further migration (Fig. 4A'). Once terminated, the neurons sent out a new prominent process to replace the leading process used during radial migration (Fig. 4A, 3:00–7:00 h), and then extended and retracted several highly dynamic processes (Figs. 4A, 7:00–15:00 h, A', 9:00–15:00 h, B, 10:00–15:00 h, and B', 5:00–9:00 h, 5). Tracking several neurons in wild-type cortices revealed that most neurons stopped their radial migration after crossing the original CP border. The neurons transitioned from a bipolar to multipolar shape and terminated at $36.8 \pm 22.3 \mu$ m above the original CP border (Fig. 4D,E).

By contrast, in *DSCAM*^{-/-} cortices, radially migrating neurons had a bipolar morphology and came to a halt within the CP (Fig. 4B, 1:00–5:00 h, B', 1:00–5:00 h). After radial migration, the neurons in *DSCAM*^{-/-} cortices might also start a nonradial migration (Fig. 4B, 6:00–9:00 h) while they transitioned from a bipolar to a multipolar shape and came to a full rest at $3.5 \pm 14.8 \mu$ m below the original CP border, almost at the original CP–MZ interface (Fig. 4B, 10:00–15:00 h, B', 5:30–9:00 h, D, E). During the course of the time-lapse imaging, the wild-type cortices expanded significantly, while the *DSCAM*^{-/-} cortices did not (Fig. 4C). Loss of *DSCAM* did not significantly alter the morphology of neurons that were terminating their radial migration (Fig. 5). These observations suggest that the positioning of nascent pyramidal neurons relative to the original CP border directly impacts the expansion of the cerebral cortex.

The developing CP border constantly moves outward during the formation of the upper cortical layer, rendering it imprecise to estimate the relative position of the expanding CP border to individually migrating neurons. Therefore, we applied a more precise method of evaluating CP outward expansion at the single-neuron resolution. This technique takes advantage of neuron pairs that migrate along the same radial axis, which enables precise measurement of the relative positions of the trailing migrating neurons to the leading migrating neurons. We fluorescently labeled pyramidal neurons using a tamoxifen-induced Nestin-Cre to drive tdTomato expression in NPCs in *DSCAM*^{+/-} and *DSCAM*^{-/-} mice. tdTomato expression was induced by a tamoxifen injection at E14.5, labeling all the nascent neurons born after E14.5, which were imaged by time-lapse microscopy.

We evaluated CP outward expansion using this system at single-neuron resolution by monitoring neuron pairs migrating along the same radial path. Under this experimental paradigm, the termination position of the leading neuron defines the outermost position of the expanding CP. The position of the trailing neuron was then measured relative to the termination position of the leading neuron to track the progress of the trailing neuron to its destination. This setup allowed us to determine at single-neuron resolution whether the trailing neuron terminates at a position before (i.e., still within the CP) or past the leading neuron (i.e., reaches the new CP to expand the upper cortical layers).

In *DSCAM*^{+/-} cortex, 67% of trailing neurons bypassed their paired leading neurons to occupy their final position beyond the original CP border (Fig. 6A,A',C,E). In contrast, in *DSCAM*^{-/-} cortex, only 11% of trailing neurons bypassed their paired leading predecessors, which instead terminated their migration adjacent to their paired leading neurons or deeper within the cortical

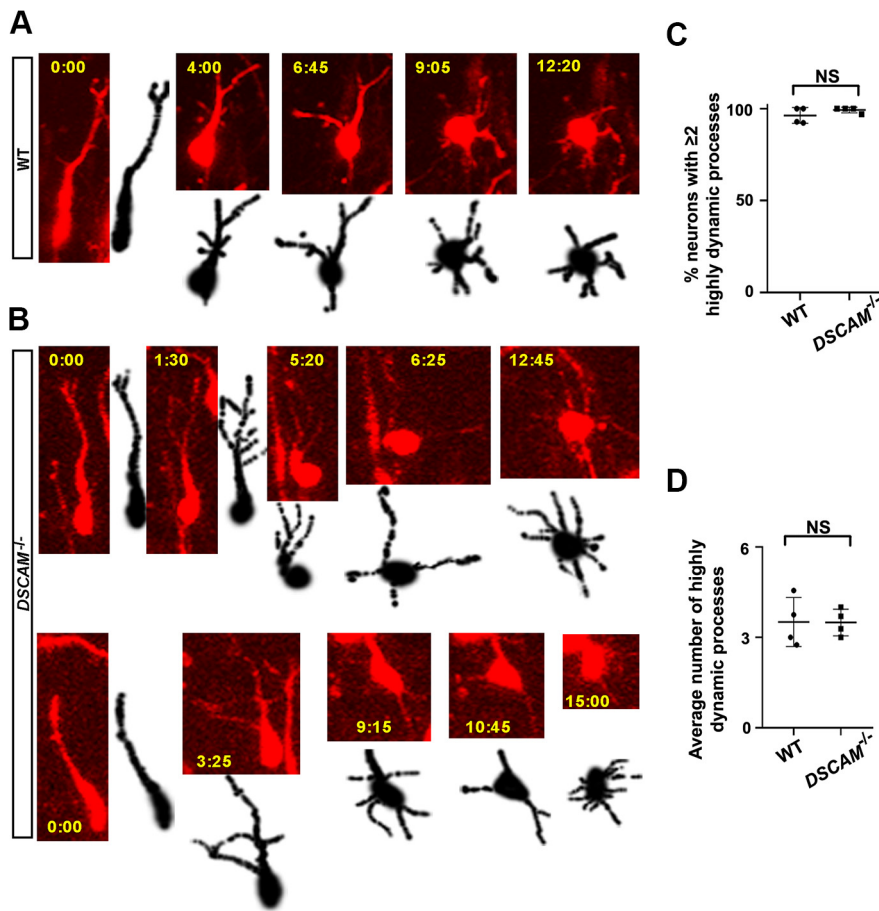


Figure 5. The morphology of neurons during the termination of radial migration. **A, B**, Time-lapse imaging shows the morphology of neurons that are terminating their radial migration in wild-type (**A**) and *DSCAM*^{-/-} (**B**) cortices at E19.5/P0. The neuron morphology was traced in black. **C, D**, Quantifications of the percentage of pyramidal neurons extending two or more highly dynamic neurites (**C**) and the average number of highly dynamic neurites (**D**) during the termination of radial migration in wild-type and *DSCAM*^{-/-} cortices at E19.5/P0. Student's *t* test. NS > 0.05.

layer (Fig. 6*B,D,E*). Furthermore, trailing neurons in *DSCAM*^{+/-} cortex terminated migration at a position further past their paired leading neurons ($14.7 \pm 13.6 \mu\text{m}$) compared with trailing neurons in *DSCAM*^{-/-} cortex ($-1.5 \pm 7.1 \mu\text{m}$; Fig. 6*F*). These results suggest that DSCAM is required by migrating pyramidal neurons to bypass their postmigratory predecessors to expand upper cortical layers.

DSCAM decreases N-cadherin-mediated adhesion in developing upper CP

How might DSCAM, as a homophilic cell adhesion molecule, facilitate the migration of pyramidal neurons to bypass their postmigratory predecessors? A previous study showed that in the mouse retina DSCAM masks cadherin-mediated cell adhesion (Garrett et al., 2018). We thus tested the possibility that DSCAM may mask or weaken adhesion from other cell adhesion molecules and therefore decrease the total cell adhesion strength in the upper CP. In this manner, DSCAM may facilitate the entry of migrating neurons into the MZ. N-cadherin is expressed throughout the CP and MZ and plays key roles in radial migration (Lai et al., 2015). To investigate the function of DSCAM in cell adhesion in the CP, we developed a HEK293T cortical slice adhesion assay. HEK293T cells express a low level of N-cadherin (Yamagata et al., 2018), which is not sufficient for mediating robust cell adhesion to brain slices (Fig.

7*A,C,D*). Nevertheless, to completely avoid a potential complication from the low level of endogenous N-cadherin in HEK293T cells, we used the HEK293NC cell line with N-cadherin knocked out, which was developed from a cloned HEK293T cell line called HEK293TA (Yamagata et al., 2018; Fig. 7*A*). Overexpressing N-cadherin in HEK293NC cells significantly increased their attachment to cortical slices (Fig. 7*C,D*). Furthermore, the adhesion of HEK293NC cells overexpressing N-cadherin to cortical slices was blocked when the cells were preincubated with a monoclonal anti-N-cadherin antibody (clone GC-4), which is known to neutralize N-cadherin function (Wallerand et al., 2010). These results suggest that the N-cadherin in HEK293NC cells and cortical slice specifically mediates the cell–cortical plate attachment.

With this test, we examined the adhesion of N-cadherin-expressing HEK293NC cells, with or without DSCAM coexpression, to cortical slices (Fig. 7*E,G–I*). HEK293NC cells expressed comparable levels of N-cadherin with or without DSCAM coexpression (Fig. 7*F*). After incubating these HEK293NC cells on wild-type brain slices, we quantified the percentages of cells attached to the MZ, upper CP, and lower CP. We found a dramatic decrease in the percentage of HEK293NC with N-cadherin and DSCAM coexpression in the upper CP (Figs. 7*E,G*), whereas the percentage of HEK293NC cells in the lower

CP and MZ were similar with or without DSCAM coexpression (Fig. 7*H,I*). These results suggest that DSCAM weakens N-cadherin-mediated cell adhesion in the developing upper CP.

We further tested this notion by replacing HEK293NC cells with pyramidal neurons dissociated from developing cortical plates. Pyramidal neurons destined to the upper cortical layers were labeled with red fluorescent protein by IUE in either *DSCAM*^{-/-} embryos or their wild-type littermates at E14.5. Then, at E19.5, dissociated neurons from transfected cortical plates were incubated with wild-type cortical slices for 2 h before fixation. *DSCAM*^{-/-} neurons attached to the upper CP significantly more than wild-type neurons (Fig. 7*J,K*). By contrast, there was no difference between *DSCAM*^{-/-} and wild-type neurons in their attachment to the lower CP and MZ (Fig. 7*L,M*). Overall, these results suggest that DSCAM weakens the attachment of migrating pyramidal neurons to the upper CP.

Discussion

The termination of neuronal radial migration is critical for cortex formation (Ohtaka-Maruyama and Okado, 2015). In this study, we found that DSCAM is involved in the termination of neuronal migration in upper cortical layers. DSCAM allows incoming nascent pyramidal neurons to bypass their predecessors at the

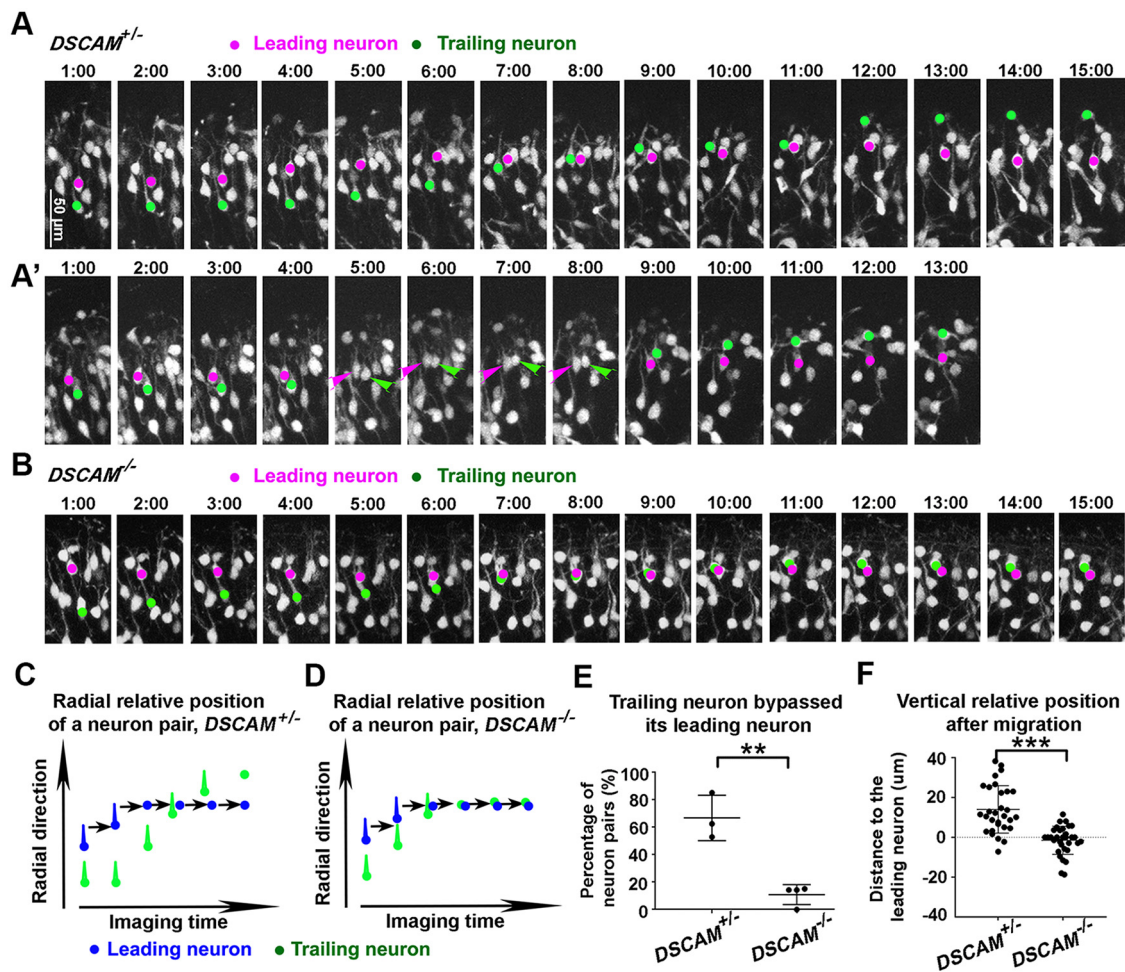


Figure 6. DSCAM is required for the trailing neurons to bypass their postmigratory predecessor neurons at the CP border. **A–B**, Representative time-lapse imaging of a pair of tdTomato⁺ migrating neurons (1 h/frame) in *DSCAM*^{+/-} (**A**, **A'**) and *DSCAM*^{-/-} (**B**) cortices in which the trailing neuron (green dots) bypasses the leading neuron (magenta dots) and attains the CP border. The green and magenta dots label the cell body positions and show the relative positions of leading and trailing neurons during the termination phase of neuronal migration. **C**, **D**, Schematics of the relative position of individual neurons of in the migrating pairs. **E**, Quantification of neuron pairs in which the trailing neuron bypasses the leading neuron in *DSCAM*^{+/-} ($n = 3$ animals) and *DSCAM*^{-/-} ($n = 4$ animals) cortex. Mann–Whitney U test, ** $p < 0.01$. **F**, Quantification of the distance between the trailing and leading neurons in *DSCAM*^{+/-} ($n = 30$ neuron pairs) and *DSCAM*^{-/-} ($n = 32$ neuron pairs). Student's t test, *** $p < 0.0001$.

CP border to expand the developing cerebral cortex. Therefore, the loss of DSCAM reduces the thickness of the upper cortical layers while increasing their neuronal density. Consistent with the selective effect on upper cortical layers in *Dscam*^{-/-} mutants, *Dscam* mRNA expression is preferentially elevated in the upper CP during upper cortical layer formation. We used the time-lapse imaging technique to demonstrate that DSCAM is required for the termination of neuronal radial migration and the determination of their final position at the CP border of the developing cortex. Through a cell adhesion assay on cortical slices, we found that DSCAM masks or weakens N-cadherin-mediated cell adhesion in the upper CP, therefore decreasing the affinity between neurons. These findings suggest that DSCAM allows the migrating neurons to bypass the CP border by masking the high-affinity cell adhesion of N-cadherin.

Radial migration of nascent pyramidal neurons in the developing cortex involves several steps. The process begins with nascent pyramidal neurons arising from NPCs in the subventricular zones, transitioning from a multipolar to a bipolar morphology before initiating the migration along radial glia. Migrating pyramidal neurons cross the SVZ, intermediate zone, and CP to terminate at the front of the developing CP, where they lose their

leading process as they come to their final position (Gongidi et al., 2004; Sanada et al., 2004; Ohtaka-Maruyama and Okado, 2015). Of all these steps, migration termination is the least understood process (Rakic, 1988; Rakic and Caviness, 1995; Gongidi et al., 2004; Ohtaka-Maruyama and Okado, 2015), despite its critical importance in cortical layer formation. The cellular and molecular underpinning of neuronal migration termination remain unknown.

We noted upper cortical layer thickness defects in the *DSCAM*^{-/-} mice. To investigate more closely, we tagged migrating pyramidal neurons with tdTomato by IUE and used *ex vivo* time-lapse imaging to monitor migration in real time. Through a quantitative analysis that we developed (Fig. 4), we found that the ability of migrating pyramidal neurons to overtake their postmigratory predecessors was impaired in *DSCAM*^{-/-} cortex. Instead, we found that *DSCAM*-deficient migrating neurons abruptly halted just at or beneath the CP border. We refined our analysis by examining neuron pairs (Fig. 6) to track relative positions more accurately. This experiment confirmed that migrating *DSCAM*^{-/-} neurons are defective in their ability to overtake the postmigratory predecessors. Importantly, our time-lapse imaging approach resolved the question of how new incoming pyramidal neurons bypass their postmigratory predecessors. Although it has been previously assumed that new

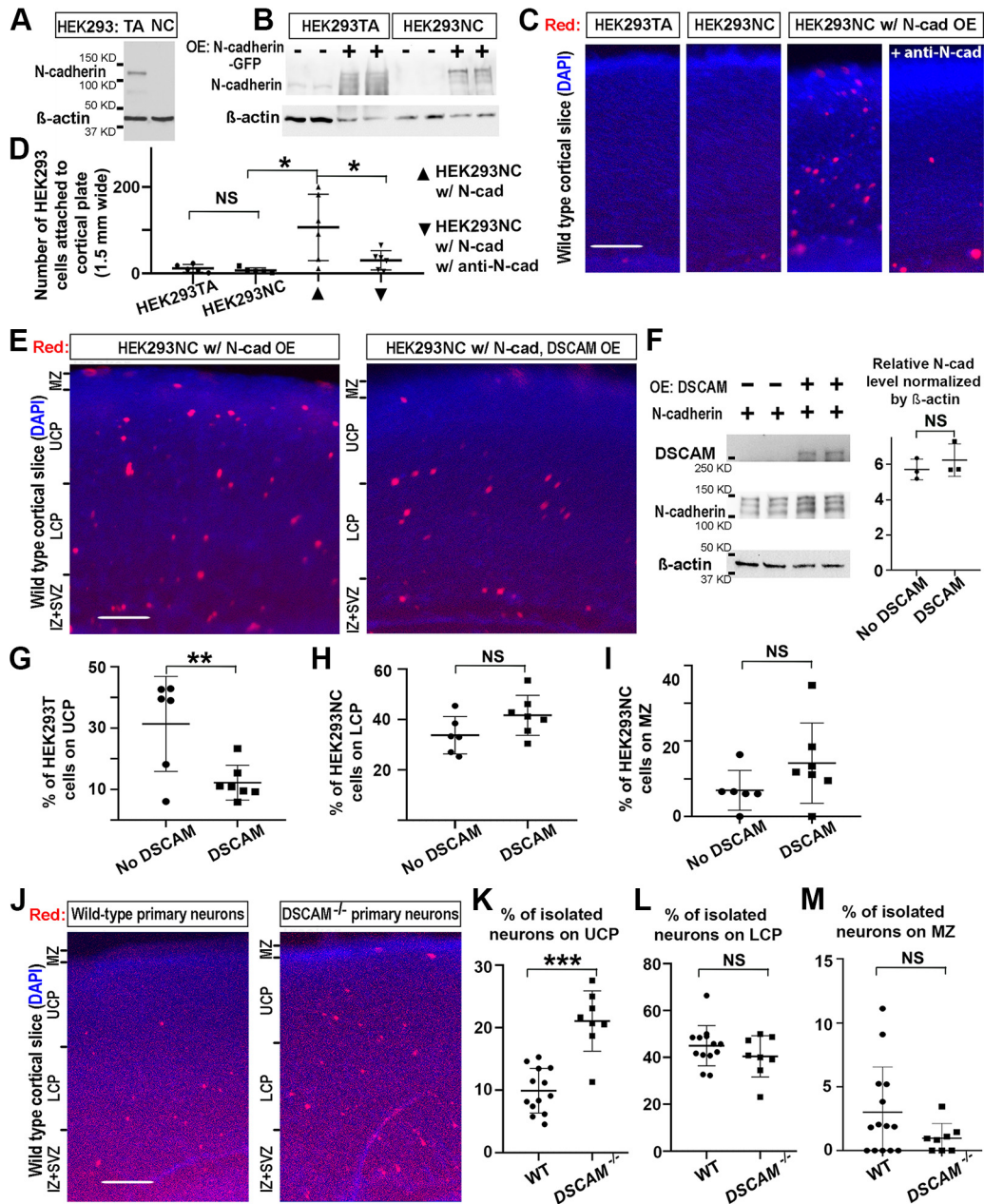


Figure 7. DSCAM decreases N-cadherin-mediated adhesion in developing upper CP. **A**, Expression of N-cadherin in HEK293TA and NC cells. **B**, Levels of N-cadherin in HEK293TA and NC cells with or without N-cadherin-GFP overexpression. **C**, **D**, While neither HEK293TA nor NC cells attach to cortical slices efficiently, overexpressing N-cadherin significantly enhances the attachment of HEK293NC to cortical slices. The attachment depends on N-cadherin because it is diminished by incubation of the HEK293 cells with an anti-N-cadherin antibody (**C**, right panel). Quantification of cells attached to E19.5 cortical slices (width, 1.5 mm) is shown in **D**. One-way ANOVA followed by *post hoc* Mann–Whitney *U* test: $NSp > 0.05$; $*p < 0.05$. Scale bar, 100 μ m. **E**, The distributions of HEK293NC cells overexpressing N-cadherin (N-Cad OE; red) on wild-type cortical slices (blue). Left, without DSCAM coexpression; right, with DSCAM coexpression. IZ, Intermediate zone; LCP, lower cortical plate; UCP, upper cortical plate; MZ, marginal zone. **F**, Western blots (left) and quantification (right) showing that overexpressing (OE) DSCAM does not affect the level of cotransfected N-cadherin. β -Actin is used as an internal control. The *y*-axis shows the ratio of N-cadherin signals to β -actin signals after background subtraction of both. Mann–Whitney *U* test. $NSp > 0.05$. **G–I**, Quantification of the percentage of HEK293NC cells adhered to the UCP (**G**), the LCP (**H**), and the MZ (**I**). Mann–Whitney *U* test: $NSp > 0.05$; $**p < 0.01$. **J**, The distributions of primary neurons (red) on wild-type cortical slices (blue). Left, The distribution of wild-type primary neurons, which expresses DSCAM. Right, The distribution of primary neurons from *DSCAM*^{-/-} mice. **K–M**, Quantification of the percentage of primary neurons adhered to the UCP (**K**), LCP (**L**), and the MZ (**M**). Mann–Whitney *U* test: $NSp > 0.05$; $***p < 0.001$.

incoming pyramidal neurons bypass postmigratory neurons to traverse the developing CP border, this study provides evidence demonstrating the role of DSCAM in this process.

Several of our observations suggest that DSCAM is required for the termination phase of radial migration but not earlier phases. First, the loss of *Dscam* reduces the thickness of upper cortical layers (layers II/III/IV) without affecting deeper cortical layer thickness (layers V/VI). Importantly, the reduction in thickness coincides with an increase in neuron density in the same layers,

suggesting a defect in neuron positioning on completing migration. Second, defects in thickness occur during upper cortical layer formation, when neurons terminate migration. Third, DSCAM expression increases at E19.5/P0, when upper cortical histogenesis begins, and especially in the nascent migrating neurons destined to form the upper cortical layer over the existing CP. On the other hand, radial migration itself was not compromised in *DSCAM*^{-/-} neurons, leaving a termination defect the likeliest explanation. This possibility motivated us to study the defect in migratory termination by *ex vivo*

time-lapse imaging, which showed significantly fewer new incoming nascent neurons bypassing their predecessors to expand the CP in *DSCAM*^{-/-} mutant.

Previous studies have shown that extracellular matrix components, such as $\alpha 3$ integrins, guide nascent pyramidal neurons as they migrate along radial glia across the entire developing cortex to the CP–MZ interface. Reelin from Cajal–Retzius cells inhibits $\alpha 3$ integrin expression to facilitate the detachment of migrating pyramidal neurons from radial glial cells (Sanada et al., 2004). Plexin A2/A4 (*PlxnA2/A4*) or Semaphorin 6A (*Sema6A*) has been proposed to play a similar role as Reelin signaling in the detachment of migrating neurons from radial glia. *Sema6A* and *PlxnA2/A4* are hypothesized to mediate a repulsive interaction between migrating neurons and radial glial cells (Hatanaka et al., 2019). Loss of *PlxnA2/A4* or *Sema6A* leads to a phenotype that resembles the Cobblestone lissencephaly (Olson and Walsh, 2002; Hatanaka et al., 2019). We found that the loss of *DSCAM* causes migrating neurons to fail to traverse the CP border, suggesting that Reelin–Dab1 and *PlxnA2/A4*–*Sema6A* signaling probably function before neurons reach the CP border. However, it is also possible that *DSCAM* functionally interacts with these signaling pathways. Clarifying these is an interesting future research direction.

DSCAM is a cell adhesion molecule primarily involved in homophilic cell adhesion (Yamakawa et al., 1998; Agarwala et al., 2000). We found that *DSCAM* is highly expressed in the developing upper CP and, surprisingly, is required by nascent pyramidal neurons to bypass the preceding neurons. This is in apparent conflict with the homophilic cell adhesion function of *DSCAM*. However, in mammals, *DSCAM* may function in concert with protocadherins (Zipursky and Sanes, 2010; Lefebvre et al., 2012) or cadherins (Garrett et al., 2018). In the mouse retina, *DSCAM*^{-/-} mutants exhibit neurite fasciculation mediated by classical cadherins (Garrett et al., 2018), suggesting a function in masking cadherin-mediated cell adhesion. *DSCAM* prevents fasciculation in a homotypic fashion, being present on both neurons. Here, we found that coexpressing *DSCAM* with N-cadherin rendered HEK293NC cells less adhesive to the upper CP of brain slices, but not the lower CP or MZ regions. These results suggest that *DSCAM* masks N-cadherin, specifically in the upper CP, allowing migrating neurons to enter the MZ. Therefore, our findings support the notion that *DSCAM* modulates adhesion strength by blocking strong cell adhesion mediated by cadherins (Garrett et al., 2018).

Previous studies have shown that the *Drosophila* homolog of *DSCAM*, *Dscam1*, mediates neurite avoidance. Whether *DSCAM* plays a similar role in migrating neurons is unknown. In the live-imaging experiments, we found that the trailing neuron bypasses the leading neuron right along each other—in some cases even contacting each other (Fig. 6A', arrowheads). This finding indicates the absence of repulsion between the migrating neurons. Moreover, although *DSCAM/Dscam1* regulates the dendrite and axon morphology of neurons, it does not seem to be required for the proper morphology of migrating neurons (Fig. 5).

In summary, we report that *DSCAM* is required for migrating neurons to bypass their postmigratory predecessors during the expansion of the upper cortical layers. This study provides insights into the proper termination of neuronal migration at the expanding border of the cortical plate. The knowledge might also help us to understand the brain disorders, which exhibit thinner cortical layers of the cerebral cortex without neuronal loss, as well as Down syndrome and autism spectrum disorders, to which *DSCAM* has been linked.

References

- Agarwala KL, Nakamura S, Tsutsumi Y, Yamakawa K (2000) Down syndrome cell adhesion molecule *DSCAM* mediates homophilic intercellular adhesion. *Brain Res Mol Brain Res* 79:118–126.
- Anton ES, Cameron RS, Rakic P (1996) Role of neuron–glial junctional domain proteins in the maintenance and termination of neuronal migration across the embryonic cerebral wall. *J Neurosci* 16:2283–2293.
- Arimura N, Okada M, Taya S, Dewa KI, Tsuzuki A, Uetake H, Miyashita S, Hashizume K, Shimaoka K, Egusa S, Nishioka T, Yanagawa Y, Yamakawa K, Inoue YU, Inoue T, Kaibuchi K, Hoshino M (2020) *DSCAM* regulates delamination of neurons in the developing midbrain. *Sci Adv* 6:eaba1693.
- Arnold SE, Trojanowski JQ (1996) Recent advances in defining the neuropathology of schizophrenia. *Acta Neuropathol* 92:217–231.
- Ayala R, Shu T, Tsai LH (2007) Trekking across the brain: the journey of neuronal migration. *Cell* 128:29–43.
- Britanova O, de Juan Romero C, Cheung A, Kwan KY, Schwark M, Gyorgy A, Vogel T, Akopov S, Mitkovski M, Agoston D, Sestan N, Molnár Z, Tarabykin V (2008) *Satb2* is a postmitotic determinant for upper-layer neuron specification in the neocortex. *Neuron* 57:378–392.
- Caviness VS Jr (1982) Neocortical histogenesis in normal and reeler mice: a developmental study based upon [3H]thymidine autoradiography. *Brain Res* 4:293–302.
- D'Arcangelo G (2006) Reelin mouse mutants as models of cortical development disorders. *Epilepsy Behav* 8:81–90.
- de Andrade GB, Long SS, Fleming H, Li W, Fuerst PG (2014) *DSCAM* localization and function at the mouse cone synapse. *J Comp Neurol* 522:2609–2633.
- Dobyns WB, Truwit CL (1995) Lissencephaly and other malformations of cortical development: 1995 update. *Neuropediatrics* 26:132–147.
- Fuerst PG, Koizumi A, Masland RH, Burgess RW (2008) Neurite arborization and mosaic spacing in the mouse retina require *DSCAM*. *Nature* 451:470–U478.
- Fuerst PG, Bruce F, Tian M, Wei W, Elstrott J, Feller MB, Erskine L, Singer JH, Burgess RW (2009) *DSCAM* and *DSCAML1* function in self-avoidance in multiple cell types in the developing mouse retina. *Neuron* 64:484–497.
- Fuerst PG, Harris BS, Johnson KR, Burgess RW (2010) A novel null allele of mouse *DSCAM* survives to adulthood on an inbred C3H background with reduced phenotypic variability. *Genesis* 48:578–584.
- Garrett AM, Khalil A, Walton DO, Burgess RW (2018) *DSCAM* promotes self-avoidance in the developing mouse retina by masking the functions of cadherin superfamily members. *Proc Natl Acad Sci U S A* 115: E10216–E10224.
- Gongidi V, Ring C, Moody M, Brekken R, Sage EH, Rakic P, Anton ES (2004) SPARC-like 1 regulates the terminal phase of radial glia-guided migration in the cerebral cortex. *Neuron* 41:57–69.
- Graham V, Khudyakov J, Ellis P, Pevny L (2003) *SOX2* functions to maintain neural progenitor identity. *Neuron* 39:749–765.
- Hatanaka Y, Kawasaki T, Abe T, Shioi G, Kohno T, Hattori M, Sakakibara A, Kawaguchi Y, Hirata T (2019) Semaphorin 6A–plexin A2/A4 interactions with radial glia regulate migration termination of superficial layer cortical neurons. *iScience* 21:359–374.
- Hattori D, Chen Y, Matthews BJ, Salwinski L, Sabatti C, Grueber WB, Zipursky SL (2009) Robust discrimination between self and non-self neurites requires thousands of *Dscam1* isoforms. *Nature* 461:644–648.
- Hughes ME, Bortnick R, Tsubouchi A, Bäumer P, Kondo M, Uemura T, Schmucker D (2007) Homophilic *Dscam* interactions control complex dendrite morphogenesis. *Neuron* 54:417–427.
- Kim JH, Wang X, Coolon R, Ye B (2013) *Dscam* expression levels determine presynaptic arbor sizes in *Drosophila* sensory neurons. *Neuron* 78:827–838.
- Kwan KY, Sestan N, Anton ES (2012) Transcriptional co-regulation of neuronal migration and laminar identity in the neocortex. *Development* 139:1535–1546.
- Lagace DC, Whitman MC, Noonan MA, Ables JL, DeCarolis NA, Arguello AA, Donovan MH, Fischer SJ, Farnbauch LA, Beech RD, DiLeone RJ, Greer CA, Mandym CD, Eisch AJ (2007) Dynamic contribution of nestin-expressing stem cells to adult neurogenesis. *J Neurosci* 27:12623–12629.
- Lai M, Guo Y, Ma J, Yu H, Zhao D, Fan W, Ju X, Sheikh MA, Malik YS, Xiong W, Guo W, Zhu X (2015) Myosin X regulates neuronal radial

- migration through interacting with N-cadherin. *Front Cell Neurosci* 9:326.
- Lefebvre JL, Kostadinov D, Chen WV, Maniatis T, Sanes JR (2012) Protocadherins mediate dendritic self-avoidance in the mammalian nervous system. *Nature* 488:517–521.
- Lin JP, Mironova YA, Shrager P, Giger RJ (2017) LRP1 regulates peroxisome biogenesis and cholesterol homeostasis in oligodendrocytes and is required for proper CNS myelin development and repair. *eLife* 6:e30498.
- Madisen L, Zwingman TA, Sunkin SM, Oh SW, Zariwala HA, Gu H, Ng LL, Palmiter RD, Hawrylycz MJ, Jones AR, Lein ES, Zeng H (2010) A robust and high-throughput Cre reporting and characterization system for the whole mouse brain. *Nat Neurosci* 13:133–140.
- Matthews BJ, Kim ME, Flanagan JJ, Hattori D, Clemens JC, Zipursky SL, Grueber WB (2007) Dendrite self-avoidance is controlled by Dscam. *Cell* 129:593–604.
- Molyneux BJ, Arlotta P, Menezes JR, Macklis JD (2007) Neuronal subtype specification in the cerebral cortex. *Nat Rev Neurosci* 8:427–437.
- Narita A, et al. (2020) Clustering by phenotype and genome-wide association study in autism. *Transl Psychiatry* 10:290.
- Nechiporuk T, Fernandez TE, Vasioukhin V (2007) Failure of epithelial tube maintenance causes hydrocephalus and renal cysts in Dlg5^{-/-} mice. *Dev Cell* 13:338–350.
- Ohtaka-Maruyma C, Okado H (2015) Molecular pathways underlying projection neuron production and migration during cerebral cortical development. *Front Neurosci* 9:447.
- Olson EC, Walsh CA (2002) Smooth, rough and upside-down neocortical development. *Curr Opin Genet Dev* 12:320–327.
- Pinto-Lord MC, Evrard P, Caviness VS Jr (1982) Obstructed neuronal migration along radial glial fibers in the neocortex of the reeler mouse: a Golgi-EM analysis. *Brain Res* 256:379–393.
- Rakic P (1988) Defects of neuronal migration and the pathogenesis of cortical malformations. *Prog Brain Res* 73:15–37.
- Rakic P, Caviness VS Jr (1995) Cortical development: view from neurological mutants two decades later. *Neuron* 14:1101–1104.
- Sanada K, Gupta A, Tsai LH (2004) Disabled-1-regulated adhesion of migrating neurons to radial glial fiber contributes to neuronal positioning during early corticogenesis. *Neuron* 42:197–211.
- Schmucker D, Chen B (2009) Dscam and DSCAM: complex genes in simple animals, complex animals yet simple genes. *Genes Dev* 23:147–156.
- Schmucker D, Clemens JC, Shu H, Worby CA, Xiao J, Muda M, Dixon JE, Zipursky SL (2000) Drosophila Dscam is an axon guidance receptor exhibiting extraordinary molecular diversity. *Cell* 101:671–684.
- Schramm RD, Li S, Harris BS, Rounds RP, Burgess RW, Ytreberg FM, Fuerst PG (2012) A novel mouse Dscam mutation inhibits localization and shedding of DSCAM. *PLoS One* 7:e52652.
- Sheldon M, Rice DS, D'Arcangelo G, Yoneshima H, Nakajima K, Mikoshiba K, Howell BW, Cooper JA, Goldowitz D, Curran T (1997) Scrambler and yotari disrupt the disabled gene and produce a reeler-like phenotype in mice. *Nature* 389:730–733.
- Soba P, Zhu S, Emoto K, Younger S, Yang SJ, Yu HH, Lee T, Jan LY, Jan YN (2007) Drosophila sensory neurons require Dscam for dendritic self-avoidance and proper dendritic field organization. *Neuron* 54:403–416.
- Sun Y, Fei T, Yang T, Zhang F, Chen YG, Li H, Xu Z (2010) The suppression of CRMP2 expression by bone morphogenetic protein (BMP)-SMAD gradient signaling controls multiple stages of neuronal development. *J Biol Chem* 285:39039–39050.
- Supèr H, Del Río JA, Martínez A, Pérez-Sust P, Soriano E (2000) Disruption of neuronal migration and radial glia in the developing cerebral cortex following ablation of Cajal-Retzius cells. *Cereb Cortex* 10:602–613.
- Tsai JW, Chen Y, Kriegstein AR, Vallee RB (2005) LIS1 RNA interference blocks neural stem cell division, morphogenesis, and motility at multiple stages. *J Cell Biol* 170:935–945.
- Turner TN, et al. (2016) Genome sequencing of autism-affected families reveals disruption of putative noncoding regulatory DNA. *Am J Hum Genet* 98:58–74.
- Verhage M, Maia AS, Plomp JJ, Brussaard AB, Heeroma JH, Vermeer H, Toonen RF, Hammer RE, van den Berg TK, Missler M, Geuze HJ, Südhof TC (2000) Synaptic assembly of the brain in the absence of neurotransmitter secretion. *Science* 287:864–869.
- Wallerand H, Cai Y, Wainberg ZA, Garraway I, Lascombe I, Nicolle G, Thierry JP, Bittard H, Radvanyi F, Reiter RR (2010) Phospho-Akt pathway activation and inhibition depends on N-cadherin or phospho-EGFR expression in invasive human bladder cancer cell lines. *Urol Oncol* 28:180–188.
- Wang T, et al. (2016) De novo genic mutations among a Chinese autism spectrum disorder cohort. *Nat Commun* 7:13316.
- Yamagata M, Sanes JR (2008) Dscam and Sidekick proteins direct lamina-specific synaptic connections in vertebrate retina. *Nature* 451:465–469.
- Yamagata M, Sanes JR (2018) Expression and roles of the immunoglobulin superfamily recognition molecule sidekick1 in mouse retina. *Front Mol Neurosci* 11:485.
- Yamagata M, Duan X, Sanes JR (2018) Cadherins interact with synaptic organizers to promote synaptic differentiation. *Front Mol Neurosci* 11:142.
- Yamakawa K, Huot YK, Haendelt MA, Hubert R, Chen XN, Lyons GE, Korenberg JR (1998) DSCAM: a novel member of the immunoglobulin superfamily maps in a Down syndrome region and is involved in the development of the nervous system. *Hum Mol Genet* 7:227–237.
- Yang T, Sun Y, Zhang F, Zhu Y, Shi L, Li H, Xu Z (2012) POSH localizes activated Rac1 to control the formation of cytoplasmic dilation of the leading process and neuronal migration. *Cell Rep* 2:640–651.
- Zipursky SL, Sanes JR (2010) Chemoaffinity revisited: dscams, protocadherins, and neural circuit assembly. *Cell* 143:343–353.
- Zou H, Li Y, Liu X, Wang X (1999) An APAF-1-cytochrome c multimeric complex is a functional apoptosome that activates procaspase-9. *J Biol Chem* 274:11549–11556.